Catalysis Science & Technology

ROYAL SOCIETY OF CHEMISTRY

PAPER

View Article Online
View Journal | View Issue

Cite this: *Catal. Sci. Technol.*, 2022, 12, 3516

A new mechanistic proposal for the aromatic cycle of the MTO process based on a computational investigation for H-SSZ-13†

Philipp N. Plessow, *[a] Annika E. Enss,[a] Philipp Huber[a] and Felix Studt [ab]

Received 5th January 2022,
Accepted 22nd April 2022

DOI: 10.1039/d2cy00021k

rsc.li/catalysis

The paring mechanism of the aromatic cycle of the hydrocarbon pool is reinvestigated based on the heptamethylbenzenium cation adsorbed within H-SSZ-13 using quantum chemical calculations. Based on the outcome of our calculations we propose a modified mechanism to that presently existing in the literature, where ring contraction starts from hexamethylmethylenecyclohexadiene. After protonation and ring contraction, the unsaturated methylene side chain remains throughout this mechanism. This new mechanistic proposal avoids the formation of antiaromatic intermediates present in current proposals for the paring mechanism. The barriers for the modified paring mechanism are found to be significantly lower than those for the original proposal, being in the range from 130–150 kJ mol^{-1} at 400 °C and are thus accessible at typical MTO conditions.

Introduction

The methanol-to-hydrocarbon (MTH) or methanol-to-olefin (MTO) process that has been discovered more than four decades ago[1] is experiencing renewed interest and growth,[2,3] as it is nowadays seen as a central pillar of our future renewable chemical industry where methanol is being produced in a sustainable way.[4,5] The process employs acidic zeotype materials and is run at temperatures of 350–400 °C. The reaction mechanism driving the conversion of methanol to a variety of differently substituted olefins, alkanes and aromatics is extremely complex and controlling product selectivities in the industrial process remains a challenge. A fundamental understanding of the mechanistic details is hence not only interesting from an academic point of view, but offers the possibility for a knowledge-based improvement of the process.

Consequently, the mechanistic details of the MTO process have been studied extensively both experimentally[6–16] and theoretically[6,16–33] and helped to establish the hydrocarbon pool concept (HPC) where olefin production has been shown to occur *via* two competing cycles with either olefins or aromatics acting as co-catalysts (see Scheme 1).[16,30,34–39] In the olefin cycle, olefins are repeatedly methylated until they are cracked into two olefins. In the aromatic cycle, aromatics are also repeatedly methylated until they eventually eliminate shorter olefins (ethene or propene).[37] The extent to which olefin and aromatic cycle contribute to the overall rate of olefin production is still under debate and likely varies for different catalysts such as H-ZSM-5,[33,40–42] H-BEA,[10,13,43–45] H-SAPO-34[19,46,47] and H-SSZ-13.[48–50] While some experimental observations involve cyclopentenyl cations,[42,51–56] all detailed mechanistic proposals for the

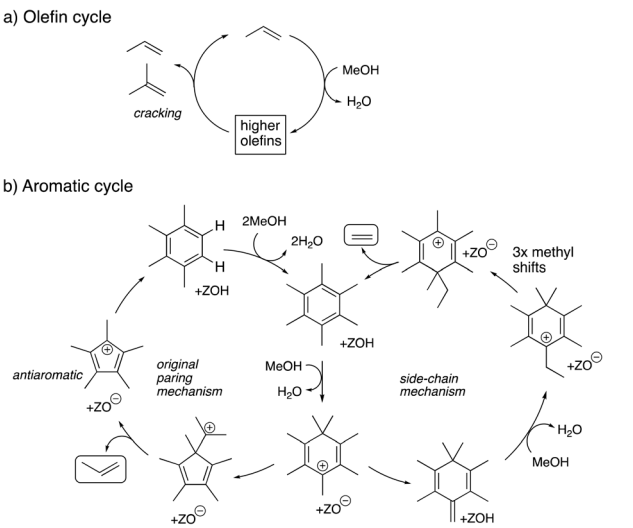

Scheme 1 Overview of the a) olefin and b) aromatic cycle of the MTO process. The aromatic cycle shown here is composed of the side-chain and paring mechanism following proposals in the literature.[37]

[a] *Institute of Catalysis Research and Technology, Karlsruhe Institute of Technology, Hermann-von-Helmholtz Platz 1, 76344 Eggenstein-Leopoldshafen, Germany. E-mail: philipp.plessow@kit.edu*

[b] *Institute for Chemical Technology and Polymer Chemistry, Karlsruhe Institute of Technology, Engesserstrasse 18, 76131 Karlsruhe, Germany*

† Electronic supplementary information (ESI) available: Additional computation information and the total energies in PDF. Structure files in XYZ and POSCAR formats are attached in the ZIP file. See DOI: https://doi.org/10.1039/d2cy00021k

aromatic cycle start from aromatic polymethylbenzenes. Two mechanistic variants have been proposed for the production of olefins *via* the aromatic cycle, the side-chain and the paring mechanism (see Scheme 1).[37]

Scheme 1 shows both mechanisms of the aromatic cycle starting from hexamethylbenzene (hexaMB). In the side-chain mechanism, hexaMB is methylated and deprotonated to form a cross-conjugated intermediate, which has an unsaturated side chain that is available for further methylation. Subsequently, this sidechain can be eliminated in the form of either ethylene or (if methylated twice) propylene. Previous computational investigations on H-SAPO-34,[19,27,46] H-ZSM-5[21] and H-SSZ-13[49] have shown that the side-chain mechanism has a clear kinetic selectivity for ethylene. These investigations, however, have also shown that the rate-limiting step, the methylation of the side chain, is relatively high with computed activation free energies on the order of 190 kJ mol^{-1} or higher as determined by us for H-SSZ-13[57] and by others for H-SAPO-34,[49,58] H-ZSM-5,[58] H-BEA[58] and H-ZSM-22.[58] We note here that in our qualitative discussion of barrier heights, we always refer to Gibbs free energies and to the highest barrier encountered in the catalytic cycle relative to the lowest preceding intermediate, thus giving the largest 'span' as described nicely in the energetic span model.[59] Individual barrier heights of elementary reaction steps, although often quoted in discussions, allow no immediate conclusion regarding the feasibility without determining the concentration of intermediates through full kinetic modeling. In some cases, a direct comparison with existing literature is therefore not possible, for example when only intrinsic barriers relative to co-adsorbed species such as methanol or water are provided.[23]

The paring mechanism is an adaptation of a related reaction observed for hydrocracking of aromatic hydrocarbons. Sullivan *et al.* coined the phrase "paring reaction" in 1961 referring to a reaction "that, in its apparent effect, peels or pares methyl groups from aromatic… rings" to produce light olefins.[60] They also proposed a mechanism involving ring expansion from five- to six-membered rings, inspired by previous reports on such reactions *via* cationic cyclopentadienyl intermediates.[61,62] Scheme 1 shows the paring mechanism adapted to the MTO process[37,39] for the heptamethylbenzenium cation (heptaMB$^+$), which contracts to a five-membered ring. This ring contraction leads to a positively charged isopropyl side chain. The next step would be the elimination of this positively charged isopropyl chain to produce propene thus leaving behind a positively charged five-membered ring. As shown in Scheme 1, this results in the formation of the pentamethylcylopentadienyl cation. Importantly, having four π-electrons, this cation is antiaromatic, violating the Hückel rule of aromaticity ($4n$ + 2 π-electrons). Both theoretical and experimental studies have found triplet ground states for substituted and unsubstituted cylopentadienyl ($C_5H_5^+$) cations,[63–65] while the penta-methylcylopentadienyl cation has not been isolated experimentally yet.[66–68] Wang *et al.* have concluded that the paring mechanism is not feasible in either H-ZSM-5 or H-SAPO-34 with barriers of 240 kJ mol^{-1} or higher.[21] This is in agreement with a recent investigation for H-SAPO-34, H-ZSM-5, H-BEA and H-ZSM-22, where barriers for the paring mechanism were always >200 kJ mol^{-1} relative to the most stable preceding adsorbate.[58]

Herein, we propose an alternative paring mechanism that avoids unfavorable antiaromatic intermediates (see Scheme 2). In our proposed mechanism, propene is eliminated from a neutral isopropyl group leading to tetramethylfulvene. We corroborate the feasibility of our mechanism using computations that are based on a hierarchical cluster approach employing periodic density functional theory (DFT) in combination with highly accurate *ab initio* calculations,[69–72] using the acidic zeolite H-SSZ-13 with hexaMB as the co-catalyst.

Results

We investigate the new variant of the paring mechanism using H-SSZ-13, which we model with periodic boundary conditions, with a unit cell containing 36 tetrahedral (T) atoms (formally Si/Al = 35). As in previous work,[72] we employ periodic DFT-calculations at the PBE-D3[73,74] level to compute minima and transition states as well as vibrations within the harmonic approximation. Using large 46T cluster models, we derive energy corrections using highly accurate *ab initio* calculations at the DLPNO-CCSD(T)[75,76] level of theory, that have been shown to accurately reproduce canonical CCSD(T).[77] The general concept of combining periodic DFT calculations with *ab initio* calculations on cluster models was pioneered in the group of Joachim Sauer and for a number of cases agreement with experimental reference values up to chemical accuracy has been demonstrated.[71] All Gibbs free energies computed in this work are given at a temperature of 400 °C and a reference pressure of 1 bar.

Scheme 2 compares the most problematic step of the original paring mechanism with the version proposed herein. In the original mechanism, propene elimination occurs without direct interaction with the acid site. In the transition

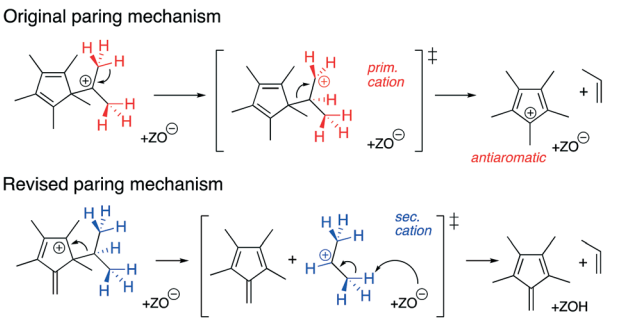

Scheme 2 Comparison of the propene-elimination step for the original paring mechanism and the revised version studied in this work.

state shown in Scheme 2, this occurs *via* a proton shift, such that a primary cation is created, followed by C–C bond cleavage, yielding free propene and the antiaromatic pentamethylcylopentadienyl cation.

In our revision of the original mechanistic proposal, propene elimination starts from a neutral isopropyl group, with the positive charge being located on the five-membered ring and with an unsaturated methylene side chain. From this precursor, propene elimination occurs in the same manner as in the side chain mechanism:[19,49,57] dissociation of the isopropyl group leads to the intermediate formation of an isopropyl cation, which is deprotonated by the anionic active site to yield free propene and the cross-conjugated intermediate tetramethylfulvene.

In our computational assessment of the original proposal of the paring mechanism for propene elimination to the

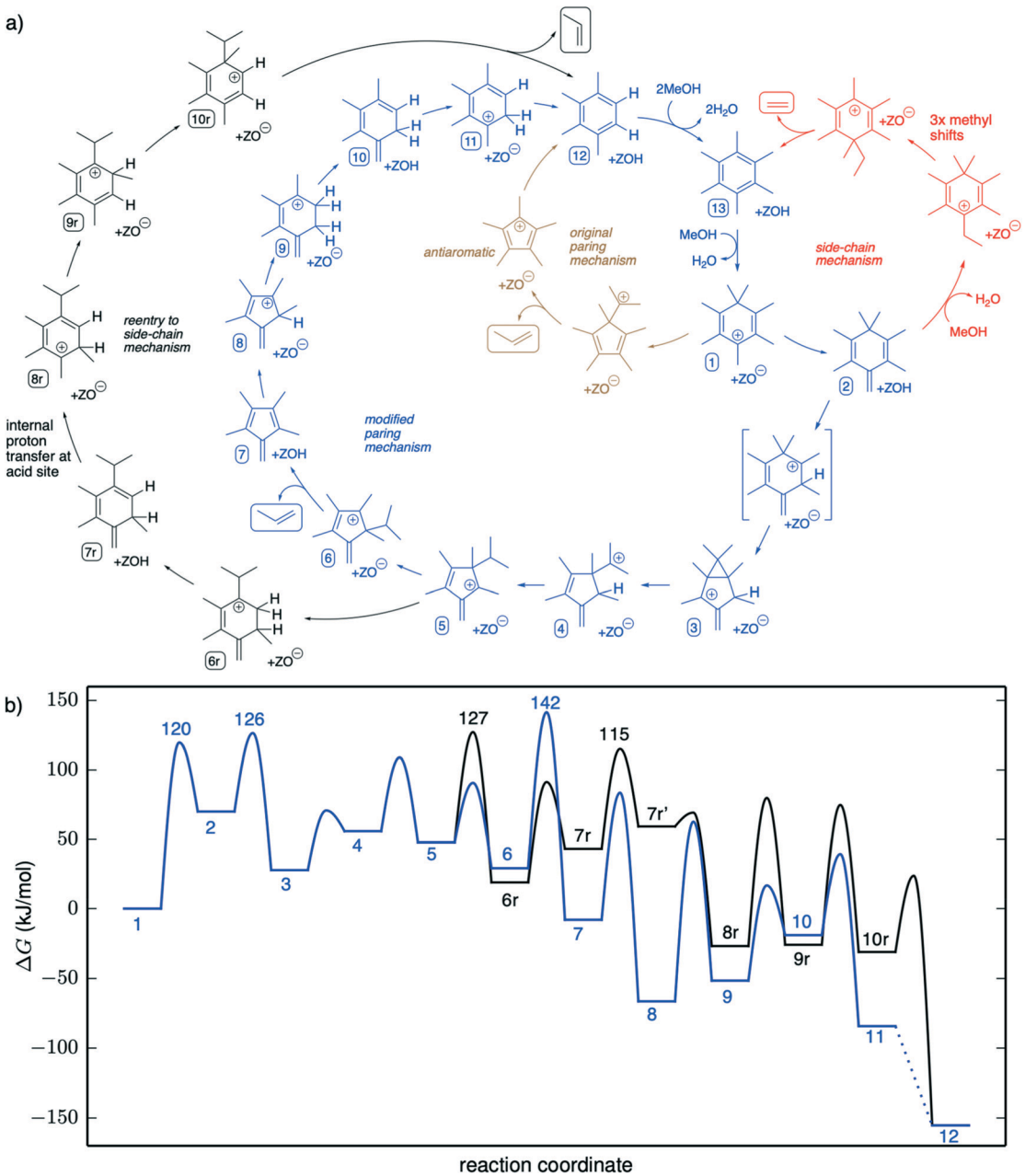

Fig. 1 Overview of the mechanistic details of the original and modified heptaMB$^+$ based aromatic cycle. a) Overview of the original paring (orange) and side-chain (red) mechanism. The detailed mechanism for the new proposal for the paring mechanism is shown in blue and includes a reentry to the side-chain mechanism (black) where elimination occurs at the six-membered ring. Accordingly, the path where propylene is eliminated from the five-membered ring is shown in blue and the path where propylene is eliminated from the six-membered ring is shown in black. b) Corresponding calculated Gibbs free energy diagram for the new proposal of the paring mechanism (color code same as in (a)) at 400 °C and 1 bar reference pressure. The adsorbates in structures 7*r* and 7*r*′ are identical, but the proton at the acid site is transferred between two different oxygens, which is facilitated by an adsorbed methanol molecule.

pentamethylcylopentadienyl cation, we find very high barriers of at least 218 kJ mol^{-1}. Our analysis shows that the adsorbate behaves indeed in the same way as the antiaromatic pentamethylcylopentadienyl cation (see ESI†). For the alternative proposal shown in Scheme 2, our calculations reveal that the depicted elimination proceeds in a single step with a modest barrier of 142 kJ mol^{-1}, relative to heptaMB$^+$. Both in the original paring mechanism, as well as in our revised version, a carbon atom from the aromatic ring is part of the released propylene. This is in contrast to the side-chain methylation and a recent study has indeed confirmed this type of mechanism using isotope labeling.[78]

Having established that our mechanistic proposal proceeds with significantly lower reaction barriers than the original paring mechanism, we will now proceed with a detailed discussion of all reaction steps of the catalytic cycle for the paring mechanism (see Fig. 1). Starting from hexaMB, heptaMB$^+$ can be formed through direct methylation with methanol. In our previous work, we have found a barrier of 150 kJ mol^{-1} for this germinal methylation.[79] Deprotonation of heptaMB$^+$ in the *para*-position gives hexamethylmethylenecyclohexadiene (HMMC) and is uphill in free energy, but requires only a moderate barrier. Methylation of HMMC (structure 2) is the rate-limiting step of the side-chain mechanism where we previously found a barrier of 206 kJ mol^{-1} relative to heptaMB$^+$ in H-SSZ-13.[57] This is in line with other findings reporting significant barriers for the side-chain mechanism.

Protonation of HMMC in the position that is *ortho* to the unsaturated side-chain leads to ring contraction as in the original proposal of the paring mechanism. The corresponding transition state TS(2–3) is shown in Fig. 2 and results in the formation of intermediate 3, where a contraction to a five-membered ring, with a fused three-membered ring occured. The three-membered ring can dissociate with a low barrier to form an isopropyl cation in the germinal-position with a methyl group (structure 4). It is noteworthy, that the specific order of these reactions depends sensitively on the orientation of the cation in the ring. Depending on small factors, such as the orientation in the pore, the protonated six-ring is a local minimum and one more barrier is required for ring contraction. For some investigated initial states, ring contraction led directly to structure 4 rather than 3. However, in all of these cases, barriers are modest and the reaction order displayed in Fig. 1 corresponds to most favorable obtained reaction path.

Starting from structure 4, an internal hydride shift from a hydrogen in a germinal position leads to a neutral isopropyl group. Importantly, the positive charge has thus shifted to the five-membered ring. From structure 5, propylene can be eliminated in the same way as in the side chain mechanism. However, the elimination reaction has been found to be more favorable from structure 6, which is formed after a shift of the isopropyl group along the 5-membered ring. In the elimination reaction, the isopropyl-group dissociates as an isopropyl cation and is concertedly deprotonated to return the proton to the active site and to give propene and the neutral, cross-conjugated five-membered ring, structure 7. This type of formation of the olefin is analogous to the side-chain mechanism[19,49,57] and also to the cracking of olefins.[80]

After protonation of structure 7 to form structure 8, ring expansion affords the six-membered ring structure 9. In the ring expansion, a methyl group in a geminal position concertedly transfers a proton to an adjacent carbon atom in the ring and the resulting CH_2-group inserts in to the C–C bond of the five-membered ring, thus expanding it to a six-membered ring. After ring expansion, a few protonation and deprotonation steps yield tetramethylbenzene (structure 12). As we have computed in previous work,[79] barriers of 163 and 157 kJ mol^{-1} are required to form hexaMB through two subsequent concerted methylation steps, thus closing the catalytic cycle.

An alternative to the discussed elimination of propylene from the five-membered ring with subsequent ring expansion is the reverse reaction order, which is shown in black in Fig. 1. Ring expansion occurs as described above, such that a methyl group is deprotonated and inserts into the five-membered ring. Compared to the initial state before ring contraction (HMMC, structure 2) where the benzene ring was fully methylated with no proton bound directly to a ring-carbon, the contraction/decontraction rearrangement steps have effectively generated an isopropyl group and replaced two methyl groups with two hydrogen atoms (structure 7r).

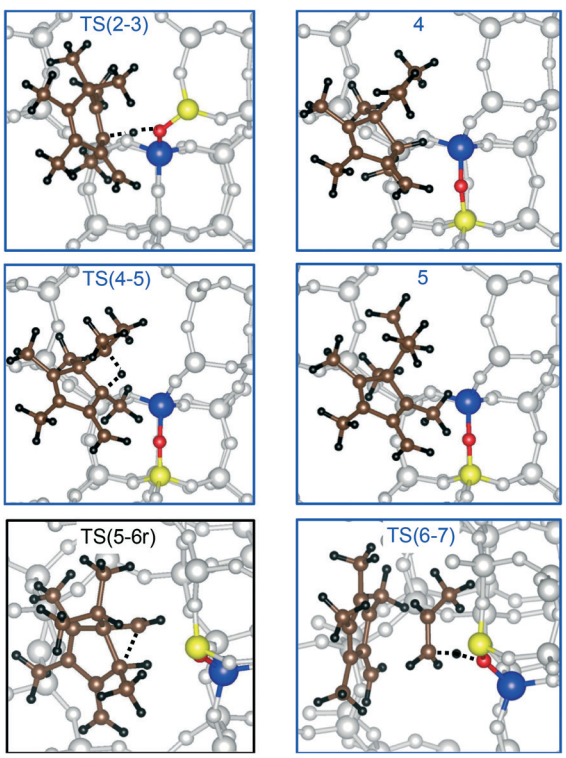

Fig. 2 Optimized structures of relevant intermediates and transition states of the paring mechanism. Color code: Si: yellow, Al: blue, O: red (remaining framework: gray), C: brown, H: black.

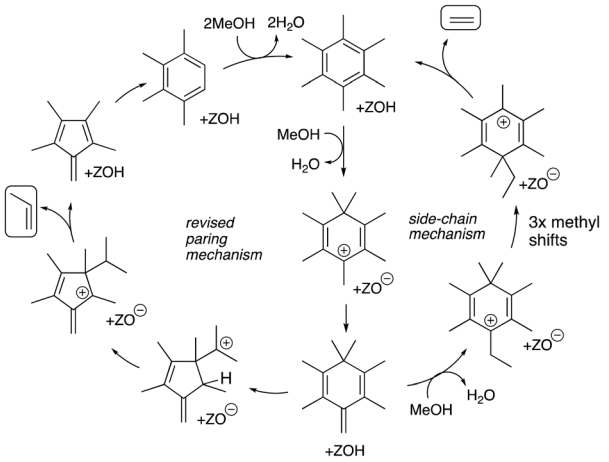

Scheme 3 Overview of the revised aromatic cycle with the herein identified new variant of the paring mechanism.

From structure 7r, a number of proton transfers and methyl shifts with relatively low barriers leads to structure 10r, which could also be generated in the side chain mechanism starting from tetramethylbenzene. In the same manner as in the side chain mechanism, elimination of propene yields tetramethylbenzene accompanied by a low barrier.

From the two possible pathways investigated here, the elimination of propylene from the six-membered ring (black pathway in Fig. 1) is slightly more favorable, with the highest barrier being 127 kJ mol^{-1} when referenced to heptaMB^{+} as the co-catalyst. This compares to 142 kJ mol^{-1} for the pathway where elimination proceeds from the 5-membered ring (blue pathway in Fig. 1). It is clear, however, that all barriers involved in our proposed version of the paring mechanism are significantly lower than those previously computed for the original paring mechanism (by more than 50 kJ mol^{-1}). Importantly, we now identified a mechanism for the entire aromatic cycle where all barriers are comparable to or lower than those commonly found for the methylation steps of aromatics (which are about 140 to 160 kJ mol^{-1}).[79] Comparing the overall energetics of propene formation *via* the paring mechanism with ethene formation *via* the side-chain mechanim,[57] shows that the paring mechanism is more favorable. We note, however, that this comparison is based on identical active site models (isolated acid sites). While our focus in this study has been on H-SSZ-13, we expect that the mechanism shown here is also the lowest energy mechanism for other zeotypes. Previous investigations have indeed shown that the original paring mechanism is unfavorable for H-ZSM-5 and H-SAPO-34[21] as well as H-BEA and H-ZSM-22,[58] thus strongly indicating that there has to be a more advantageous pathway for propylene formation with lower overall free energies.

Conclusions

We presented a new mechanistic proposal for the paring mechanism of the aromatic cycle of the methanol-to-olefins process. We used a computational protocol that yields highly accurate reaction barriers and investigated the new mechanism using acidic H-SSZ-13 as the catalyst. Scheme 3 gives a concise summary of the aromatic cycle with the revised paring mechanism proposed in this contribution.

Importantly, this revised paring mechanism involves ring contraction to the five-membered ring from hexamethylmethylenecyclohexadiene protonated in the *ortho* position relative to the methylidene group, rather than starting directly from the heptamethylbenzenium cation as originally proposed. This mechanism thus avoids the formation of antiaromatic species and the elimination of propylene from a primary cationic precursor. Our proposed mechanism is hence calculated to proceed *via* a pathway with significantly lower overall free energy reaction barriers than that originally proposed. In fact, our results reveal that the paring mechanism exhibits barriers comparable to or even lower than those commonly computed for the methylation of aromatic species, which we found to be typically in the range of 140 to 160 kJ mol^{-1} for H-SSZ-13, using the same methodology.[79]

The proposed mechanism can thus explain why propylene is formed in high quantities in the MTO process. In contrast, the original paring mechanism has too high barriers to be relevant while the side-chain mechanism is selective towards ethylene and the olefin cycle is selective towards branched olefins that can be formed *via* tertiary carbocations. We thus report for the first time a comprehensive mechanism of propylene formation. This in-depth understanding of the processes that govern the MTO process will allow the knowledge-based improvement of acidic zeotype catalysts.

Computational details

All structures were optimized with PBE-D3[73,74] (zero damping) using the projector-augmented wave method[81] as implemented in VASP[82,83] in version 5.4.1 with standard PAW potentials and a plane-wave basis set with an energy cutoff of 400 eV for the wave function, Gaussian smearing with a width of 0.1 eV and k-point sampling only at the Γ-point. In calculations on gas phase molecules and clusters, these species were separated by at least 16 Å of vacuum. The lattice constants (a = b = 13.625 Å, c = 15.067 Å) of CHA were optimized in previous work using an increased energy cutoff of 800 eV. Transition state searches were performed using automated relaxed potential energy surface scans (ARPESS),[84] as implemented in a local version of the atomic simulation environment (ASE).[85] Additionally, the nudged elastic band (NEB)[86] and the dimer method[87] have been used, mainly to investigate barriers for rotation of the adsorbate. Transition states were verified to contain only a single imaginary frequency corresponding to the transition mode. The connectivity of transition states was verified through distortion along the eigenmode followed by minimization to the adjacent minima. Free energies were computed using the harmonic approximation based on a partial Hessian that includes the adsorbates and the Si–O–Al

fragment of the acid site. Harmonic frequencies below 12 cm^{-1} were raised to this value to reduce errors from the harmonic approximation. Gas phase molecules were additionally treated according to the rigid rotator and free translator approximation. All Gibbs free energies reported are obtained at 400 °C and 1 bar reference pressure.

Additional *ab initio* calculations were performed on cluster models to increase the accuracy of the computed energies. The 46T cluster model for the single-site case is the same as in previous work[72] and was cut from the zeolite framework, where the terminating Si–O bonds were substituted with Si–H bonds pointing along the original Si–O direction, with a fixed Si–H bond length of 1.489 Å. Single-point energy calculations were then carried out for the cluster model and the final energy is obtained as:

$$E = E^{\mathrm{PBC}}_{\mathrm{PBE\text{-}D3}} + E^{\mathrm{cluster}}_{ab\ initio} - E^{\mathrm{cluster}}_{\mathrm{PBE\text{-}D3}},$$

$$E^{\mathrm{cluster}}_{ab\ initio} = E^{\mathrm{cluster}}_{\mathrm{CCSD(T)/DZ}} + E^{\mathrm{cluster}}_{\mathrm{MP2/CBS}} - E^{\mathrm{cluster}}_{\mathrm{MP2/DZ}}.$$

Here, all CCSD(T) and MP2 calculations employ the DLPNO-approximation[75,76] and were carried out with ORCA in version 4.2.1 using the "TightPNO" threshold setting. The PBE-D3 calculations on the cluster models were carried out with VASP with the same setups as for the periodic models. Complete basis set (CBS) extrapolation was carried separately for MP2-correlation using the cc-pVXZ basis sets with X = D, T with the two point l^{-3}-formula[88] and for the Hartree–Fock energy using the three point exponential formula with X = D, T, Q.[89] Hartree–Fock calculations with ORCA employ the RIJCOSX approximation using appropriate basis sets for RI and the X6 grid for the chain-of-spheres exchange (COSX).[90]

Author contributions

The manuscript was written through contributions of all authors. All authors have given approval to the final version of the manuscript.

Conflicts of interest

The authors declare no competing financial interests.

Acknowledgements

The authors acknowledge support by the state of Baden-Württemberg bwHPC (bwunicluster and JUSTUS, RV bw17D011). Financial support from the Helmholtz Association is also gratefully acknowledged. Gefördert durch die Deutsche Forschungsgemeinschaft (DFG) – Projektnummer 434253773.

Notes and references

1 C. D. Chang and W. H. Lang, *US Pat.*, US4025576A, 1977.
2 I. Yarulina, A. D. Chowdhury, F. Meirer, B. M. Weckhuysen and J. Gascon, *Nat. Catal.*, 2018, **1**, 398–411.
3 P. Tian, Y. Wei, M. Ye and Z. Liu, *ACS Catal.*, 2015, **5**, 1922–1938.
4 G. A. Olah, *Angew. Chem., Int. Ed.*, 2005, **44**, 2636–2639.
5 G. A. Olah, *Angew. Chem., Int. Ed.*, 2013, **52**, 104–107.
6 D. M. McCann, D. Lesthaeghe, P. W. Kletnieks, D. R. Guenther, M. J. Hayman, V. Van Speybroeck, M. Waroquier and J. F. Haw, *Angew. Chem., Int. Ed.*, 2008, **47**, 5179–5182.
7 T. Mole, J. A. Whiteside and D. Seddon, *J. Catal.*, 1983, **82**, 261–266.
8 B. Arstad and S. Kolboe, *J. Am. Chem. Soc.*, 2001, **123**, 8137–8138.
9 B. Arstad and S. Kolboe, *Catal. Lett.*, 2001, **71**, 209–212.
10 A. Sassi, M. A. Wildman, H. J. Ahn, P. Prasad, J. B. Nicholas and J. F. Haw, *J. Phys. Chem. B*, 2002, **106**, 2294–2303.
11 W. Song, J. F. Haw, J. B. Nicholas and C. S. Heneghan, *J. Am. Chem. Soc.*, 2000, **122**, 10726–10727.
12 M. Bjørgen, F. Bonino, S. Kolboe, K.-P. Lillerud, A. Zecchina and S. Bordiga, *J. Am. Chem. Soc.*, 2003, **125**, 15863–15868.
13 M. Bjørgen, U. Olsbye, D. Petersen and S. Kolboe, *J. Catal.*, 2004, **221**, 1–10.
14 M. Bjørgen, U. Olsbye, S. Svelle and S. Kolboe, *Catal. Lett.*, 2004, **93**, 37–40.
15 W. Dai, X. Wang, G. Wu, N. Guan, M. Hunger and L. Li, *ACS Catal.*, 2011, **1**, 292–299.
16 K. Hemelsoet, J. Van der Mynsbrugge, K. De Wispelaere, M. Waroquier and V. Van Speybroeck, *ChemPhysChem*, 2013, **14**, 1526–1545.
17 D. Lesthaeghe, A. Horré, M. Waroquier, G. B. Marin and V. Van Speybroeck, *Chem. – Eur. J.*, 2009, **15**, 10803–10808.
18 B. Arstad, J. B. Nicholas and J. F. Haw, *J. Am. Chem. Soc.*, 2004, **126**, 2991–3001.
19 C.-M. Wang, Y.-D. Wang and Z.-K. Xie, *Catal. Sci. Technol.*, 2014, **4**, 2631–2638.
20 C.-M. Wang, Y.-D. Wang, H.-X. Liu, Z.-K. Xie and Z.-P. Liu, *Microporous Mesoporous Mater.*, 2012, **158**, 264–271.
21 C.-M. Wang, Y.-D. Wang, Y.-J. Du, G. Yang and Z.-K. Xie, *Catal. Sci. Technol.*, 2016, **6**, 3279–3288.
22 C.-M. Wang, Y.-D. Wang, Z.-K. Xie and Z.-P. Liu, *J. Phys. Chem. C*, 2009, **113**, 4584–4591.
23 K. De Wispelaere, K. Hemelsoet, M. Waroquier and V. Van Speybroeck, *J. Catal.*, 2013, **305**, 76–80.
24 D. Lesthaeghe, B. De Sterck, V. Van Speybroeck, G. B. Marin and M. Waroquier, *Angew. Chem., Int. Ed.*, 2007, **46**, 1311–1314.
25 Y. Chu, X. Sun, X. Yi, L. Ding, A. Zheng and F. Deng, *Catal. Sci. Technol.*, 2015, **5**, 3507–3517.
26 C.-M. Wang, Y.-D. Wang, Y.-J. Du, G. Yang and Z.-K. Xie, *Catal. Sci. Technol.*, 2015, **5**, 4354–4364.
27 C.-M. Wang, Y.-D. Wang, H.-X. Liu, Z.-K. Xie and Z.-P. Liu, *J. Catal.*, 2010, **271**, 386–391.
28 S. Wang, Y. Chen, Z. Wei, Z. Qin, H. Ma, M. Dong, J. Li, W. Fan and J. Wang, *J. Phys. Chem. C*, 2015, **119**, 28482–28498.
29 C.-M. Wang, Y.-D. Wang, H.-X. Liu, G. Yang, Y.-J. Du and Z.-K. Xie, *Chin. J. Catal.*, 2015, **36**, 1573–1579.

30 V. Van Speybroeck, K. De Wispelaere, J. Van der Mynsbrugge, M. Vandichel, K. Hemelsoet and M. Waroquier, *Chem. Soc. Rev.*, 2014, **43**, 7326–7357.
31 C. Chizallet, *ACS Catal.*, 2020, 5579–5601, DOI: **10.1021/acscatal.0c01136**.
32 G. Li and E. A. Pidko, *ChemCatChem*, 2018, **11**, 134–156.
33 I. Yarulina, K. De Wispelaere, S. Bailleul, J. Goetze, M. Radersma, E. Abou-Hamad, I. Vollmer, M. Goesten, B. Mezari, E. J. M. Hensen, J. S. Martinez-Espin, M. Morten, S. Mitchell, J. Perez-Ramirez, U. Olsbye, B. M. Weckhuysen, V. Van Speybroeck, F. Kapteijn and J. Gascon, *Nat. Chem.*, 2018, **10**, 804–812.
34 I. M. Dahl and S. Kolboe, *Catal. Lett.*, 1993, **20**, 329–336.
35 I. M. Dahl and S. Kolboe, *J. Catal.*, 1994, **149**, 458–464.
36 I. M. Dahl and S. Kolboe, *J. Catal.*, 1996, **161**, 304–309.
37 U. Olsbye, S. Svelle, M. Bjorgen, P. Beato, T. V. Janssens, F. Joensen, S. Bordiga and K. P. Lillerud, *Angew. Chem., Int. Ed.*, 2012, **51**, 5810–5831.
38 V. Van Speybroeck, K. Hemelsoet, L. Joos, M. Waroquier, R. G. Bell and C. R. Catlow, *Chem. Soc. Rev.*, 2015, **44**, 7044–7111.
39 J. F. Haw, W. Song, D. M. Marcus and J. B. Nicholas, *Acc. Chem. Res.*, 2002, **36**, 317–326.
40 I. Yarulina, S. Bailleul, A. Pustovarenko, J. R. Martinez, K. D. Wispelaere, J. Hajek, B. M. Weckhuysen, K. Houben, M. Baldus, V. Van Speybroeck, F. Kapteijn and J. Gascon, *ChemCatChem*, 2016, **8**, 3057–3063.
41 D. Lesthaeghe, A. Horre, M. Waroquier, G. B. Marin and V. Van Speybroeck, *Chemistry*, 2009, **15**, 10803–10808.
42 C. Wang, Y. Chu, A. Zheng, J. Xu, Q. Wang, P. Gao, G. Qi, Y. Gong and F. Deng, *Chemistry*, 2014, **20**, 12432–12443.
43 A. Sassi, M. A. Wildman and J. F. Haw, *J. Phys. Chem. B*, 2002, **106**, 8768–8773.
44 M. Bjørgen, *J. Catal.*, 2003, **215**, 30–44.
45 M. Bjørgen, U. Olsbye, S. Svelle and S. Kolboe, *Catal. Lett.*, 2004, **93**, 37–40.
46 C. M. Wang, Y. D. Wang, Z. K. Xie and Z. P. Liu, *J. Phys. Chem. C*, 2009, **113**, 4584–4591.
47 C.-M. Wang, Y.-D. Wang and Z.-K. Xie, *J. Catal.*, 2013, **301**, 8–19.
48 F. Bleken, M. Bjorgen, L. Palumbo, S. Bordiga, S. Svelle, K. P. Lillerud and U. Olsbye, *Top. Catal.*, 2009, **52**, 218–228.
49 C. M. Wang, Y. D. Wang, Y. J. Du, G. Yang and Z. K. Xie, *Catal. Sci. Technol.*, 2015, **5**, 4354–4364.
50 S. Xu, A. Zheng, Y. Wei, J. Chen, J. Li, Y. Chu, M. Zhang, Q. Wang, Y. Zhou, J. Wang, F. Deng and Z. Liu, *Angew. Chem., Int. Ed.*, 2013, **52**, 11564–11568.
51 P. Ferri, C. Li, C. Paris, A. Vidal-Moya, M. Moliner, M. Boronat and A. Corma, *ACS Catal.*, 2019, **9**, 11542–11551.
52 E. D. Hernandez, B. Manookian, S. M. Auerbach and F. C. Jentoft, *ACS Catal.*, 2021, 12893–12914, DOI: **10.1021/acscatal.1c03039**.
53 T. Xu and J. F. Haw, *J. Am. Chem. Soc.*, 2002, **116**, 7753–7759.
54 J. F. Haw, J. B. Nicholas, W. Song, F. Deng, Z. Wang, T. Xu and C. S. Heneghan, *J. Am. Chem. Soc.*, 2000, **122**, 4763–4775.
55 D. Xiao, X. Han, X. Bao, G. Hou and F. Blanc, *RSC Adv.*, 2019, **9**, 12415–12418.
56 M. J. Wulfers and F. C. Jentoft, *ACS Catal.*, 2014, **4**, 3521–3532.
57 M. Fečík, P. N. Plessow and F. Studt, *Catal. Sci. Technol.*, 2021, **11**, 3826–3833.
58 Y. Chen, S. Wang, Z. Wei, J. Li, M. Dong, Z. Qin, J. Wang and W. Fan, *J. Phys. Chem. C*, 2021, **125**, 26472–26483.
59 S. Kozuch and S. Shaik, *Acc. Chem. Res.*, 2011, **44**, 101–110.
60 R. F. Sullivan, C. J. Egan, G. E. Langlois and R. P. Sieg, *J. Am. Chem. Soc.*, 1961, **83**, 1156–1160.
61 L. De Vries, *J. Am. Chem. Soc.*, 1960, **82**, 5242–5244.
62 S. Winstein and M. Battiste, *J. Am. Chem. Soc.*, 1960, **82**, 5244–5245.
63 M. Saunders, R. Berger, A. Jaffe, J. M. McBride, J. O'Neill, R. Breslow, J. M. Hoffmann, C. Perchonock, E. Wasserman, R. S. Hutton and V. J. Kuck, *et al.*, *J. Am. Chem. Soc.*, 1973, **95**, 3017–3018.
64 W. J. Hehre and P. V. R. Schleyer, *J. Am. Chem. Soc.*, 1973, **95**, 5837–5839.
65 R. Breslow, H. W. Chang, R. Hill and E. Wasserman, *J. Am. Chem. Soc.*, 1967, **89**, 1112–1119.
66 M. Otto, D. Scheschkewitz, T. Kato, M. M. Midland, J. B. Lambert and G. Bertrand, *Angew. Chem., Int. Ed.*, 2002, **41**, 2275–2276.
67 T. Muller, *Angew. Chem., Int. Ed.*, 2002, **41**, 2276–2278.
68 J. B. Lambert, L. Lin and V. Rassolov, *Angew. Chem., Int. Ed.*, 2002, **41**, 1429–1431.
69 S. Svelle, C. Tuma, X. Rozanska, T. Kerber and J. Sauer, *J. Am. Chem. Soc.*, 2009, **131**, 816–825.
70 N. Hansen, T. Kerber, J. Sauer, A. T. Bell and F. J. Keil, *J. Am. Chem. Soc.*, 2010, **132**, 11525–11538.
71 J. Sauer, *Acc. Chem. Res.*, 2019, **52**, 3502–3510.
72 P. N. Plessow and F. Studt, *J. Phys. Chem. Lett.*, 2020, **11**, 4305–4310.
73 J. P. Perdew, K. Burke and M. Ernzerhof, *Phys. Rev. Lett.*, 1996, **77**, 3865–3868.
74 S. Grimme, J. Antony, S. Ehrlich and H. Krieg, *J. Chem. Phys.*, 2010, **132**, 154104.
75 C. Riplinger, B. Sandhoefer, A. Hansen and F. Neese, *J. Chem. Phys.*, 2013, **139**, 134101.
76 C. Riplinger and F. Neese, *J. Chem. Phys.*, 2013, **138**, 034106.
77 C. Riplinger, P. Pinski, U. Becker, E. F. Valeev and F. Neese, *J. Chem. Phys.*, 2016, **144**, 024109.
78 A. Hwang, B. A. Johnson and A. Bhan, *J. Catal.*, 2019, **369**, 86–94.
79 M. Fečík, P. N. Plessow and F. Studt, *ACS Catal.*, 2020, **10**, 8916–8925.
80 P. N. Plessow and F. Studt, *Catal. Sci. Technol.*, 2018, **8**, 4420–4429.
81 P. E. Blochl, *Phys. Rev. B: Condens. Matter*, 1994, **50**, 17953–17979.
82 G. Kresse and J. Furthmüller, *Phys. Rev. B: Condens. Matter Mater. Phys.*, 1996, **54**, 11169–11186.
83 G. Kresse and D. Joubert, *Phys. Rev. B: Condens. Matter Mater. Phys.*, 1999, **59**, 1758–1775.
84 P. N. Plessow, *J. Chem. Theory Comput.*, 2018, **14**, 981–990.

85 A. Hjorth Larsen, J. Jorgen Mortensen, J. Blomqvist, I. E. Castelli, R. Christensen, M. Dulak, J. Friis, M. N. Groves, B. Hammer, C. Hargus, E. D. Hermes, P. C. Jennings, P. Bjerre Jensen, J. Kermode, J. R. Kitchin, E. Leonhard Kolsbjerg, J. Kubal, K. Kaasbjerg, S. Lysgaard, J. Bergmann Maronsson, T. Maxson, T. Olsen, L. Pastewka, A. Peterson, C. Rostgaard, J. Schiotz, O. Schutt, M. Strange, K. S. Thygesen, T. Vegge, L. Vilhelmsen, M. Walter, Z. Zeng and K. W. Jacobsen, *J. Phys.: Condens. Matter*, 2017, **29**, 273002.
86 G. Henkelman and H. Jónsson, *J. Chem. Phys.*, 2000, **113**, 9978–9985.
87 G. Henkelman and H. Jonsson, *J. Chem. Phys.*, 1999, **111**, 7010–7022.
88 T. Helgaker, W. Klopper, H. Koch and J. Noga, *J. Chem. Phys.*, 1997, **106**, 9639–9646.
89 D. Feller, *J. Chem. Phys.*, 1992, **96**, 6104–6114.
90 F. Neese, F. Wennmohs, A. Hansen and U. Becker, *Chem. Phys.*, 2009, **356**, 98–109.